Genomics

Molecular Cancer Research

MiR-335 Inhibits Small Cell Lung Cancer Bone Metastases via IGF-IR and RANKL Pathways

Meng Gong[1,2], Junrong Ma[1,2], Ryan Guillemette[2], Mingliang Zhou[1], Yan Yang[1], Yujing Yang[1], Janet M. Hock[2], and Xijie Yu[1,2]

Abstract

Small cell lung cancer (SCLC) is a rapidly progressing, incurable cancer that frequently spreads to bone. New insights are needed to identify therapeutic targets to prevent or retard SCLC metastatic progression. Human SCLC SBC-5 cells in mouse xenograft models home to skeletal and nonskeletal sites, whereas human SCLC SBC-3 cells only pervade nonskeletal sites. Because microRNAs (miRNA) often act as tumor regulators, we investigated their role in preclinical models of SCLC. miRNA expression profiling revealed selective and reduced expression of miRNA (miR)-335 and miR-29a in SBC-5 cells, compared with SBC-3 cells. In SBC-5 cells, miR-335 expression correlated with bone osteolytic lesions, whereas miR-29a expression did not. Overexpression of miR-335 in SBC-5 cells significantly reduced cell migration, invasion, proliferation, colony formation, and osteoclast induction *in vitro*. Importantly, in miR-335 overexpressing SBC-5 cell xenografts ($n = 10$), there were minimal osteolytic lesions in the majority of mice and none in three mice. Expression of RANK ligand (RANKL) and insulin-like growth factor-I receptor (IGF-IR), key mediators of bone metastases, were elevated in SBC-5 as compared with SBC-3 cells. Mechanistically, overexpression of miR-335 in SBC-5 cells reduced RANKL and IGF-IR expression. In conclusion, loss of miR-335 promoted SCLC metastatic skeletal lesions via deregulation of IGF-IR and RANKL pathways and was associated with metastatic osteolytic skeletal lesions.

Implications: These preclinical findings establish a need to pursue the role of miR-335 in human SCLC with metastatic skeletal disease. *Mol Cancer Res; 12(1); 101–10. ©2013 AACR.*

Introduction

Small cell lung cancer (SCLC), a highly aggressive form of lung cancer associated with tobacco smoking (1, 2), represents 10% to 15% of all lung cancers (3, 4). Treatment is challenging because SCLC grows rapidly, often becoming well established in lung before becoming symptomatic; metastatic spread occurs early and rapidly (5, 6). For patients with localized or regionalized SCLC, 5-year survival in the United States in 2008 was 52% and 25%, respectively (7). For those who suffer metastatic SCLC or relapse, the prognosis is worse. Although there have been advances in therapy for localized SCLC with the introduction of positron emission tomography, SCLC mortality has remained unchanged over the past 30 years (6).

Compared with our knowledge of skeletal metastases in breast and prostate cancers, we know very little about cell and molecular mechanisms of skeletal metastases in lung cancer, especially in SCLC. In osteolytic lesions, such as those in breast cancer, bone loss predominates, while increased bone turnover in which both bone formation and bone resorption are deregulated, is characteristic of skeletal metastases in prostate cancer (8, 9). More than one third of patients with SCLC develop osteolytic bone metastasis, resulting in severe pain, pathologic fractures, spinal cord compression, and loss of mobility to greatly reduce the quality of life (10, 11). Because of the lack of therapeutic options in SCLC, there is an urgent need to better understand how skeletal progression in SCLC may be controlled and treated.

microRNAs (miRNA) critically regulate tumorigenesis and progression by targeting oncogenes, tumor suppressor genes, or genes related to proliferation, angiogenesis, and apoptosis. miRNAs are a class of small noncoding RNAs of about 19 to 25 nucleotides (nt) that function as negative posttranscriptional gene regulators (12, 13). By hybridizing to the 3′ untranslated region (UTR) of target mRNAs, miRNAs can serve as mediators of mRNA cleavage and cause translational repression, or act on transcription to

Authors' Affiliations: [1]Laboratory of Endocrinology and Metabolism, State Key Laboratory of Biotherapy, West China Hospital, Sichuan University, Sichuan, People's Republic of China; and [2]Maine Institute for Human Genetics & Health, Brewer, Maine

Note: Supplementary data for this article are available at Molecular Cancer Research Online (http://mcr.aacrjournals.org/).

Corresponding Author: Xijie Yu, MD, PhD, Laboratory of Endocrinology and Metabolism, State Key Laboratory of Biotherapy, West China Hospital, Sichuan University, No. 37 Guoxue Xiang, Chengdu, Sichuan 610041, People's Republic of China. Phone: 86-28-8542-2362; Fax: 86-28-8542-3459; E-mail: xijieyu@hotmail.com

doi: 10.1158/1541-7786.MCR-13-0136

reduce protein output by destabilizing mRNAs (14). Different tumor types and tumors at various differentiation stages may exhibit unique miRNA profiles (15). In non–small cell lung cancer (NSCLC) cells, miRNA (miR)-494, miR-30a, miR-193b, miR-101, miR-7, and miR-206 have been reported as tumor inhibitors (16–21), whereas miR-212 is believed to promote carcinogenesis *in vitro* (22). In patients with NSCLC, high miR-155 and low let-7a-2 expression in tumor tissue have been reported to correlate with poor survival (23). Unfortunately, miRNAs, which have been associated with clinical outcomes in metastatic NSCLC, have not been found relevant to SCLC (24). More research is needed to investigate the selectivity and specificity of miRNA pathways in SCLC and its metastatic spread to bone, and their possible value as therapeutic targets to improve survival.

Human SBC-5 and SBC-3 cell lines were originally established from human SCLC, and found to differ in their predilection for bone when tested as xenografts in immunodeficient mice (25, 26). Xenografts of SBC-5 or SBC-3 cells formed multiple tumor foci in liver, pancreas, ovary/uterus, and kidney in natural killer (NK)-depleted immunodeficient mouse models. SBC-5 cell xenografts promoted osteolytic bone lesions, whereas SBC-3 cell xenografts did not (25, 26). We previously reported a more consistent immunodeficient mouse host model for xenografts of bone metastases, using human SCLC SBC-5 cells injected into the tail vein of nonobese diabetic/severe combined immunodeficient (NOD/SCID) $IL2R_{\gamma}^{null}$ mice, deficient in T cells, B cells, and NK cells (27). SBC-5 and SBC-3 xenografts homed to multiple nonskeletal tissues, such as liver, pancreas, uterus, ovary, and kidney, and formed lesions that were indistinguishable in location and morphology (27). Osteolytic bone lesions were observed throughout the skeleton of mice with SBC-5 cell xenografts, whereas no bone lesions were observed in mice with SBC-3 cell xenografts (27). We applied this model to study skeletal progression of SCLC in the preclinical studies reported here.

Our goal was to investigate miRNAs involved in the regulation of skeletal metastatic SCLC lesions. A comparison of miRNA profiles of SBC-5 with SBC-3 cell lines revealed selective downregulation in miR-335 and miR-29a in SBC-5 cells. Overexpression of miR-335, but not miR-29a, in SBC-5 cells decreased cell proliferation, colony formation, migration and invasion, and osteoclast induction *in vitro*, and prevented or reduced osteolytic metastases *in vivo*.

Materials and Methods

Ethics statement

This study was approved by the Ethics Committees of West China Hospital of Sichuan University (Sichuan, People's Republic of China). Experiments in the United States involving mice were reviewed and approved by The Jackson Laboratory Institutional Animal Care and Use Committee.

Cell culture

Human SCLC SBC-5 and SBC-3 cell lines (SBC-5 and SBC-3, respectively) were obtained from the Japan Health Sciences Foundation, Health Science Resources Bank (HSRB; JCRB0819 and JCRB0818), and authenticated by DNA short tandem repeats profile assay. SBC-5 and SBC-3 were maintained in advanced Dulbecco's modified Eagle medium (DMEM) medium (Invitrogen) supplemented with 10% FBS (Thermo-Hyclone). Human kidney cell line, 293TN, was purchased from SBI (System Biosciences) and maintained in advanced DMEM medium with 10% FBS.

Analysis of miRNA expression by microarray and qRT-PCR

RNA was extracted from cells using an RNeasy miRNA kit (Qiagen Inc.,). miRNA microarrays were conducted by LC Sciences. The miRNA microarrays included 833 human miRNAs, representing miRNA transcripts listed in Sanger miRBase Release 11.0. The microarrays included four independent RNA samples from each cell line. To ensure accuracy of the hybridizations, each RNA sample was hybridized with three membranes. Hybridization signals for each spot of the array and background values at 15 empty spots were measured. Hybridization signals that failed to exceed the average background value by more than three SD were excluded from analysis. Signal intensities for each spot were calculated by subtracting the background values from the total intensities. Data normalization was conducted using positive control RNA spots [tRNA(G), tRNA(L), tRNA(T), tRNA(H), and 5S rRNA] to allow comparisons among chips. The remaining data were averaged among triplicate arrays, and the resulting four datasets, each corresponding to an RNA sample, were considered independent measurements for the purposes of paired, two-sample *t* test when comparing miRNA profiles in SBC-5 with SBC-3.

Reverse transcriptase (RT) and quantitative real-time PCR were conducted in a two-step reaction using Taqman miRNA assays according to the protocol provided by the manufacturer (Applied Biosystems). U6 was used as the internal control. The $2^{-\Delta\Delta Ct}$ method described by Livak and Schmittgen (28) was used to analyze the data.

Stable overexpression of miR-335 or miR-29a in the SBC-5 cell line

A lentiviral expression system was used to establish stable SBC-5 cell lines with high miR-335 or miR-29a expression. Lenti-miR-335 or Lenti-miR-29a miRNA Precursor Expression Construct (System Biosciences) was used to prepare lentivirus with the LentiSuite (System Biosciences) according to the manufacturer's protocol. The pGreenPuro Scramble Hairpin Control Construct (System Biosciences) was used to prepare control lentivirus. Lentiviral infection was conducted according to the manufacturer's protocol. Transfected cells were trypsinized, diluted in culture medium, and seeded in 96-well plate at one cell/well in average. After 7-day culture, single-cell colonies with high fluorescence were chosen out and cultured to be stable cell lines. Quantitative reverse transcriptase PCR (qRT-PCR) was used to assay the expression of miR-335 or miR-29a in these stable cell lines. The SBC-5 cell lines with highest miR-335 expression (named as SBC-5 miR-335^{+}) or miR-29a

expression (named as SBC-5 miR-29a$^+$) were selected for the assays described in the following sections. SBC-5 cells transfected with control lentivirus were used as control cell line (named as SBC-5 Vector^{Ctrl}) for *in vitro* and *in vivo* experiments.

Cell migration and invasion

SBC-5 miR-335$^+$, SBC-5 miR-29a$^+$, and SBC-5 Vector^{Ctrl} cell lines were serum starved for 24 hours, trypsinized and resuspended in 0.1% FBS-supplemented medium with no additional growth factors. SBC-5 cells were plated at a density of 1×10^4 cells/well in a Transwell insert (3 μm pore size, BD Biosciences) for the migration assay, and in a Matrigel-coated, growth factor-reduced invasion chamber (8 μm pore size, BD Biosciences) for the invasion assay. Ten percent FBS-containing medium was added into 24-well plates to provide a chemoattractant. After 6-hour incubation for the migration assay or after 22-hour incubation for the invasion assay, cells were fixed with 4% paraformaldehyde for 1 hour. Cells on the apical side of each insert were removed by mechanically scraping. Cells located on the basal side of the membrane were stained with 0.1% crystal violet, and visualized under a Zeiss Axiovert 200M microscope. Cell numbers were quantified using Metamorph analysis software.

MTT proliferation assay

SBC-5 miR-335$^+$, SBC-5 miR-29a$^+$, and SBC-5 Vector^{Ctrl} cell lines were cultured to 70% to 80% confluence, serum starved for 24 hours, and then cultured at a density of 1,500 cells/well in 96-well plates with advanced DMEM medium supplemented with 2% FBS at 5% CO_2, 37ºC. At selected time points, MTT was added at a final concentration of 0.5 mg/mL. After 4-hour incubation at 37ºC, medium was removed, and purple blue sediment was dissolved in 150 μL of dimethyl sulfoxide. The relative optical density for each well was determined using a Wellscan MK3 ELISA kit (Labsystems) as a measure of proliferation.

Colony formation

SBC-5 miR-335$^+$, SBC-5 miR-29a$^+$, and SBC-5 Vector^{Ctrl} cell lines were seeded at a density of 100 cells/dish in 60 mm dishes, and cultured for 14 days. Cells were fixed with 4% paraformaldehyde for 20 minutes, and stained with 0.1% crystal violet for 30 minutes. Colony numbers were counted using bright-field microscopy.

Osteoclast induction assay, using SBC-5 conditioned media

SBC-5 miR-335$^+$, SBC-5 miR-29a$^+$, and SBC-5 Vector^{Ctrl} cell lines were cultured to 90% confluence, washed with PBS, and incubated at 37°C for 24 hours in advanced DMEM with 0.5% FBS. Incubation supernatants from each SBC-5 cell line were harvested, and conditioned media (CM) were prepared as 10% incubation supernatant, 10% FBS, 80% α-MEM, 10 ng/mL macrophage colony-stimulating factor (M-CSF), and 10 ng/mL RANK ligand (RANKL) for each cell line. Cell-free unconditioned medium was constituted as 90% α-MEM with 10% FBS, 10 ng/mL M-CSF, and 10 ng/mL RANKL. For osteoclast induction assays, spleen cells from 4-week-old C57BL mice (strain: C57BL/6J, Jackson Laboratory) were prepared, using the method described by Granholm and colleagues (29). The cells were seeded in 24-well plate at 1×10^7/well, and cultured in conditioned or unconditioned media. Cells were cultured for 7 days, with media replaced every 2 days. On the final day, cells were fixed in 4% paraformaldehyde and stained for TRAP (tartrate-resistant acid phosphatase) using Acid Phosphatase, Leukocyte (TRAP) Kit (Sigma-Aldrich). TRAP$^+$ cells with 3 or more nuclei were counted under brightfield microscopy, and expressed as number of osteoclasts/well.

Western blotting

Cells were lysed in radioimmunoprecipitation assay (RIPA) buffer containing Halt Protease Inhibitor Cocktail (Pierce). Protein concentration was determined with Quick Start Bradford Protein Assay kit (Bio-Rad). The blotting membrane was incubated overnight at 4°C with different primary antibodies: anti-IGF-IR (1:1000; Abcam), anti-RANKL (1:500; Epitomics), and anti-β-actin (1:1000; Sigma). The blots were incubated for 1 hour at room temperature with either horseradish peroxidase-conjugated secondary antibody: anti-mouse or anti-rabbit immunoglobulin (Chemicon). Signals were visualized using enhanced chemiluminescence plus chemiluminescence substrate (Amersham).

RANKL 3′UTR reporter assay

The potential miR-335 target site predicted by miRanda on RANKL mRNA 3′UTR was amplified from human genomic DNA using the primer pair(forward: 5′- GTCTGGAGAGGAAATCAGCATCGA-3′; reverse: 5′-TTCAGATGATCCTTCAATTGCGCT-3′)and subcloned into the pMIR-REPORT miRNA reporter vector (Ambion). Recombined plasmids were confirmed by DNA sequencing. Point mutation within the target sequence for miR-335 in 3′UTR (3′UTRm) was generated by the QuickChange II XL site-directed mutagenesis kit (Stratagene) using primers (forward: 5′-TATCCATAAGGTTGACCTTGTAGAGAACACGCGTAT-3′ and 5′-AAGGTCAACCTTATGGATACTGAGTCGTGTACCGT-3′). The plasmid containing 3′ UTRm was sequenced to confirm replacement of the targeted residues. Lentivirus was used to stably transfect miR-335 precursor gene or control sequence into 293TN cells. Transfected cells were further cotransfected via a pMIR reporter vector with RANKL 3′UTR fragment, or corresponding mutation fragment together with the pMIR-REPORT β-galactosidase reporter control vector (Ambion). Cells were collected at 24 hours after transfection. The ratio of β-galactosidase to firefly luciferase was measured with Dual Luciferase Assay kit (Promega).

SCLC skeletal metastases model

Immunodeficient mice, NOD/SCID IL2R$_\gamma^{null}$ (strain: NOD.Cg-Prkdc^{scid} Il2r^{gtm1Wjl}/SzJ; Jackson Laboratory),

were housed as 2 to 5 same sex mice in polycarbonate cages (324 cm^2) at The Jackson Laboratory under barrier conditions. Mice were maintained under 14:10-hour light: dark cycles; provided sterilized White Pine shavings for bedding, and fed with NIH 31 irradiated diet (6% fat, 19% protein, Ca:P of 1.15:0.85), with vitamin and mineral fortification (Purina Mills International), and sterilized water *ad libitum*.

SBC-5 miR-335$^+$, SBC-5 miR-29a$^+$, and SBC-5 Vector^{Ctrl} were cultured under equivalent conditions. Cells were harvested at about 80% confluence, washed with ice-cold PBS twice, and resuspended in cold PBS at a density of 5×10^6 cells/mL. On day 0, the cell suspension was injected at 1×10^6 cells per mouse via tail vein injection into 8-week-old NOD/SCID IL2R$_\gamma^{null}$ male mice (10 mice per group). Mice were euthanized on day 28, and their bodies were fixed in 10% neutralized formalin for at least 2 days. Radiographs of the skeleton were taken with a Faxitron MX20 cabinet X-ray (Faxitron X-Ray Corp.,) and Kodak Min-R 2000 mammography film (Eastman Kodak Co.,). Skeletal osteolytic lesions observed in radiographs were counted in the spine, right and left femurs, and tibias and ulnar bones.

Statistical analysis

Analyses were conducted with JMP 8.0 software (SAS). We used ANOVA to compare multiple groups, followed by pairwise comparisons if significant differences were detected. Tukey–Kramer test was used for comparisons with a control group. Dunnett test was used to compare all groups. Unpaired *t* tests were used to compare data when only two groups were used. Differences were considered statistically significant at $P < 0.05$ on a two-tailed test. Data were expressed as mean ± SEM.

Results

Reduced expression of miR-335 and miR-29a in SBC-5 cells compared with SBC-3 cells

Prior work reports that SBC-5 cells colonize skeletal and nonskeletal tissues, whereas SBC-3 cells only colonize nonskeletal tissues. This fact indicates that SBC-5 cells may produce specific factors to communicate with osteoclasts and/or osteoblasts to colonize into skeleton. Indeed a few factors, such as PTHrP and CCR4, have been reported to be upregulated in SBC-5 cells (30, 31). The molecular mechanisms under upregulation of these factors are not clear. As miRNAs function as negative posttranscriptional gene regulators, we hypothesize that selective and specific miRNAs are expressed reductively in SBC-5 cells, which induce upregulation of the bone-communicating factors. In the primary screen, 14 miRNAs, including miR-9, miR-10a, miR-17–92 family, miR-29 family, and miR-335, were expressed at lower levels in SBC-5 than in SBC-3 (fold change >2, $P < 0.001$; Table 1; Supplementary Materials and Methods and Supplementary Fig. S1). Because microarray data reflect relative differences in miRNA expression patterns of SBC-5 and SBC-3, we determined whether candidate miRNAs were also present in human normal lung tissues. Compared with normal lung tissue, miR-335 and miR-29a expression was lower in SBC-5 cells, whereas no changes were observed for the other miRNAs. On the basis of these observations, we focused on miR-335 and miR-29a and excluded the other miRNAs (Fig. 1).

Overexpression of miR-335, but not miR-29a, reduces *in vitro* carcinogenesis

Using a lentiviral transfection strategy, miR-335 or miR-29a genes were stably transfected into SBC-5, respectively.

Table 1. Significantly decreased miRNAs in SBC-5, compared with SBC-3

Name	Average intensity in SBC-3	Average intensity in SBC-5	Fold change	*P*
hsa-miR-29c	614.57	305.34	2.013	0.001793
hsa-miR-29b	3,080.87	1,498.71	2.056	0.000111
hsa-miR-29a	2,279.61	1,043.33	2.185	0.000101
hsa-miR-10a	1,303.50	489.89	2.661	5.00E-06
hsa-miR-20b	1,999.95	348.05	5.746	4.00E-07
hsa-miR-19a	5,356.96	805.51	6.650	3.00E-07
hsa-miR-9	2,296.92	336.93	6.817	1.00E-07
hsa-miR-92a	2,530.69	364.94	6.935	7.00E-07
hsa-miR-17	4,236.43	593.20	7.142	2.00E-07
hsa-miR-17-3p	565.45	70.72	7.995	8.00E-07
hsa-miR-18b	480.99	59.82	8.041	1.10E-06
hsa-miR-18a	1,572.21	165.96	9.473	<1e-07
hsa-miR-335-3p	4,528.73	2.53	1,788.642	1.00E-07
hsa-miR-335	2,937.27	1.00	2,937.272	<1e-07

NOTE: miRNA profiles in human SBC-5 and SBC-3 were conducted by using the miRNA microarrays (833 human miRNAs). Four replicates of each cell line were analyzed in each microarray. Compared with SBC-3 cells, 14 miRNAs in SBC-5 cells were decreased by more than 2-fold ($P < 0.001$).

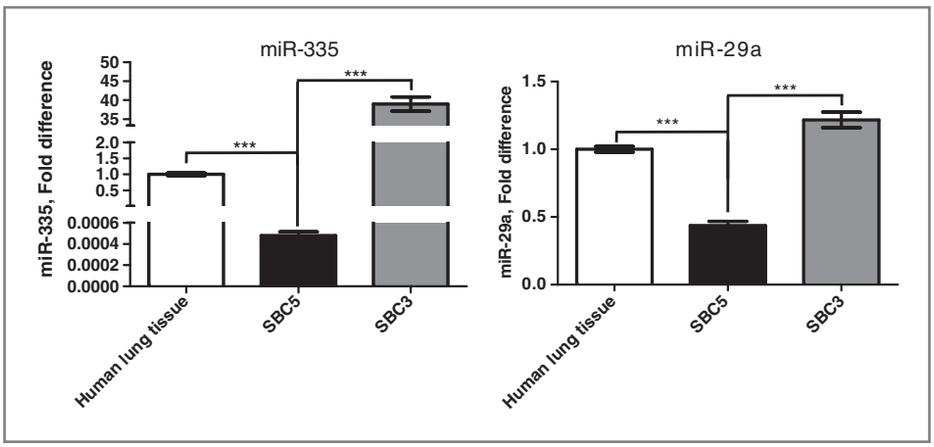

Figure 1. Comparison of miR-335 and miR-29a expression in human SCLC SBC-5 and SBC-3 cells. Validation of miR-335 and miR-29a by qRT-PCR confirmed the miRNA array profiles as both miRNAs were significantly lower in SBC-5 cell, than in SBC-3 or in normal human lung tissue (***, $P < 0.001$; $n = 5$/group).

The lentivirus system enabled external miRNA gene expression from the constitutive cytomegalovirus promoter and contained copGFP as a reporter. Lentiviral transfection of SBC-5 was successful, exhibiting a robust transfection rate (>90%). To obtain stable cell lines with high expression of the selected miRNA, we screened GFP expression in single colonies in 96-well plates, and verified miRNA expression by qRT-PCR. Transfection of *miR-335* gene in SBC-5 (SBC-5 miR-335$^+$) increased miR-335 expression by more than 2,600-fold, compared with control lentivirus-transfected

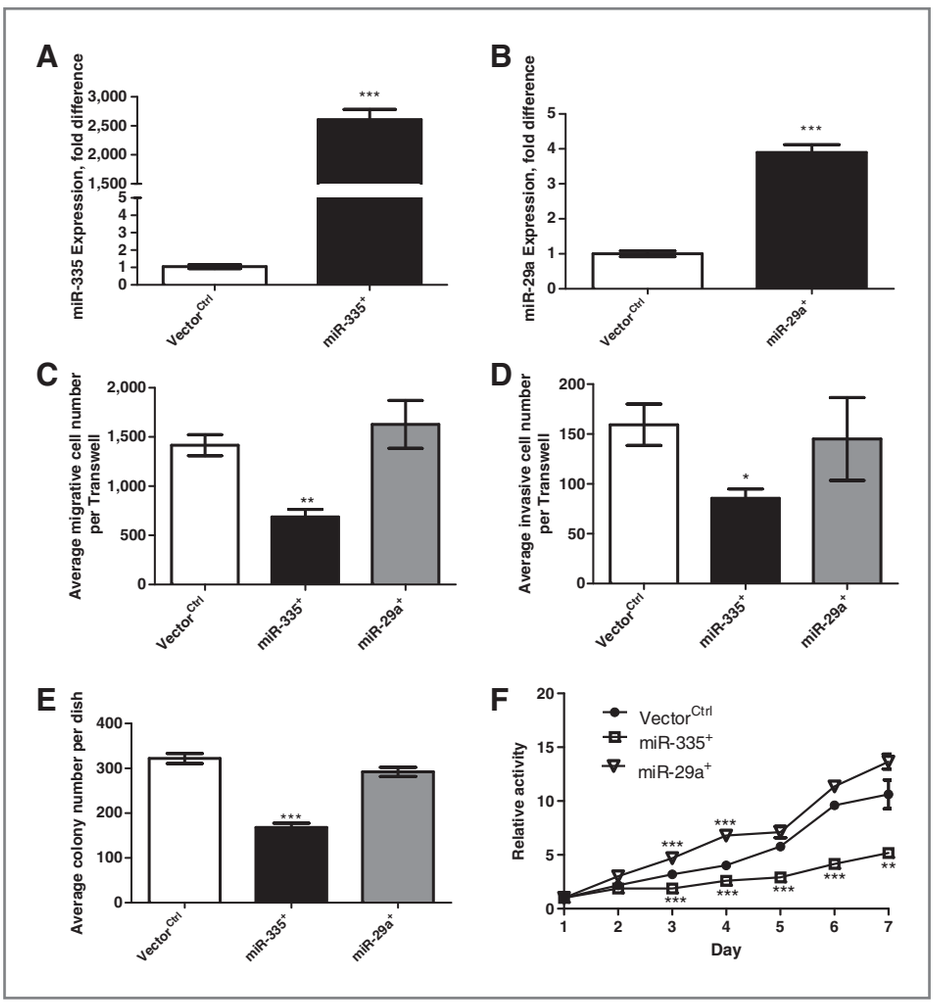

Figure 2. Overexpression of miR-335, but not miR-29a, reduces *in vitro* carcinogenesis. A and B, stable transfection of SBC-5 cells to overexpress miR-335 or miR-29a was achieved using a lentiviral system. Screening of single colonies by qRT-PCR was used to select cell lines with the highest expression of miR-335 (SBC-5 miR-335$^+$) or miR-29a (SBC-5 miR-29a$^+$; $n = 3$/group) for subsequent studies. Stable SBC-5 cell line transfected with control lentivirus was used as control cell line (SBC-5 Vector^{Ctrl}). C and D, compared with SBC-5 Vector^{Ctrl} cells, cell migration and invasion were significantly reduced in SBC-5 miR-335$^+$ cells, but not in SBC-5 miR-29a$^+$ cells ($n = 3$/group, 2 replicate experiments). E, SBC-5 miR-335$^+$ formed fewer colonies than SBC-5 Vector^{Ctrl}, whereas SBC-5 miR-29a$^+$ was equivalent to SBC-5 Vector^{Ctrl} ($n = 3$/group, two replicate experiments). F, proliferation, assessed by the MTT assay, was lower in SBC-5 miR-335$^+$ than that in SBC-5 Vector^{Ctrl}, whereas proliferation of SBC-5 miR-29a$^+$ cells was equivalent or slightly increased compared with SBC-5 Vector^{Ctrl} cells ($n = 5$/group/time point, 3 replicate experiments; compared with control, *, $P < 0.05$; **, $P < 0.01$; ***, $P < 0.001$).

SBC-5 (SBC-5 Vector^{Ctrl}), that expressed very little miR-335 (Fig. 2A; $P < 0.001$). SBC-5 expressed miR-29a at relatively high levels. Transfection of *miR-29a* gene in SBC-5 increased miR-29a expression only by approximately 4-fold compared with controls (Fig. 2B; $P < 0.001$).

In migration and invasion assays *in vitro*, miR-335 overexpression in SBC-5 miR-335$^+$ reduced cell migration by approximately 52% (average cell number per well, SBC-5 miR-335$^+$: 687 ± 77 vs. SBC-5 Vector^{Ctrl}: 1416 ± 107; $P < 0.01$; Fig. 2C) and cell invasion by approximately 46% (average invasive cell number per well, SBC-5 miR-335$^+$: 86 ± 9 vs. SBC-5 Vector^{Ctrl}: 159 ± 21; $P < 0.05$; Fig. 2D). In colony formation assay, because of metastatic nature, SBC-5 cells adhere poorly to plastic and proliferating cells and often drift away from their original colonies to form additional colonies, so SBC-5 colony number usually exceeds the number of cells plated after 2-week culture. MiR-335 overexpression in SBC-5 miR-335$^+$ reduced cell colony formation by approximately 48% (average colony number per dish, SBC-5 miR-335$^+$: 168 ± 10 vs. SBC-5 Vector^{Ctrl}: 322 ± 11; $P < 0.001$; Fig. 2E). In contrast, cell migration, cell invasion, and colony formation of SBC-5 miR-29$^+$ did not differ significantly from SBC-5 Vector^{Ctrl} (Fig. 2C–E). Compared with SBC-5 Vector^{Ctrl}, SBC-5 miR-335$^+$ exhibited significantly lower proliferation from culture on day 3, whereas proliferation of SBC-5 miR-29a$^+$ did not differ from SBC-5 Vector^{Ctrl}, except for a slight increase on days 3 and 4 of culture (Fig. 2F). Collectively, these data suggested that miR-335 overexpression reduced the potential for metastatic cancer progression by inhibiting cell migration, invasion, proliferation, and colony formation. In contrast, miR-29a overexpression did not modify key aspects of SBC-5 functional phenotype.

Xenografts of SBC-5 miR-335$^+$, but not SBC-5 miR-29a$^+$, abrogated skeletal lesions *in vivo*

"Metastatic" spread to skeletal and nonskeletal tissues was observed following intravenous tail injections of SBC-5 Vector^{Ctrl} xenograft. Radiographs showed SBC-5 Vector^{Ctrl} xenografts induced osteolytic bone lesions in the spine and long bones. In mice with SBC-5 miR-335$^+$ xenografts, skeletal osteolytic lesions were absent in 3 mice and reduced overall (average number of lesions/mouse: 1.3 ± 0.36 vs. SBC-5 Vector^{Ctrl}: 3.3 ± 0.42; $P < 0.01$; Fig. 3). Four mice with either SBC-5 miR-335$^+$ or SBC-5 miR-29a$^+$ xenografts, each exhibited 1 osteolytic lesion, whereas the remaining 3 mice with miR-335$^+$ xenografts exhibited 3 osteolytic lesions each. Mice with SBC-5 miR-29a$^+$ or Vector^{Ctrl} xenografts exhibited 2 or more (3–5) lesions each, in 6 and

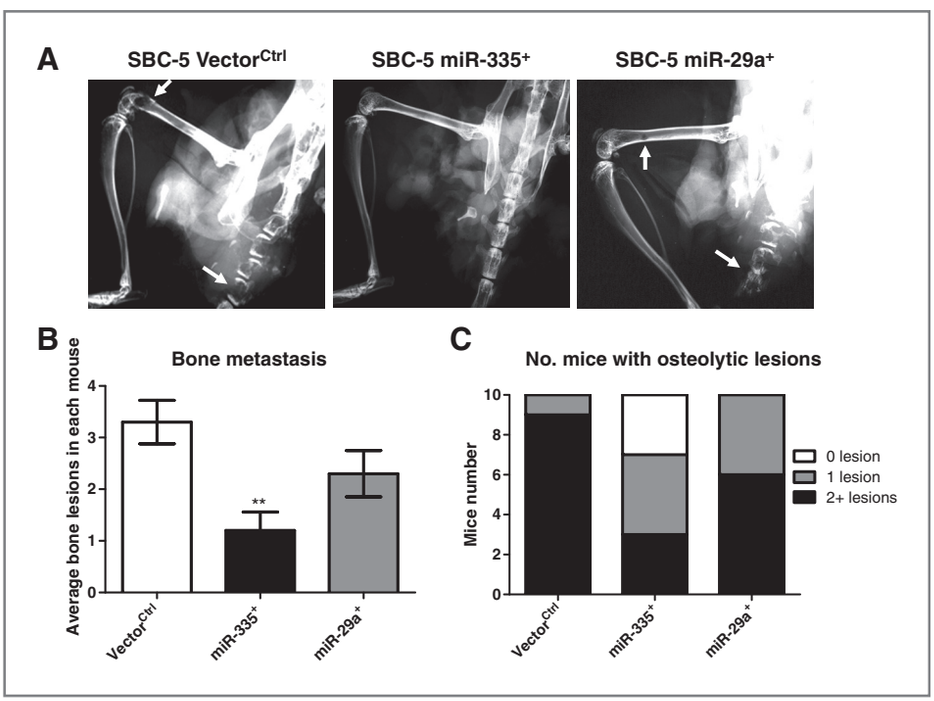

Figure 3. SBC-5 miR-335$^+$ xenografts abrogated completely, or in part, skeletal osteolytic lesions in humanized NOD/SCID IL2R$_\gamma^{null}$ immunodeficient mice. SBC-5 miR-335$^+$ cells, SBC-5 miR-29a$^+$ cells, or control (SBC-5 Vector^{Ctrl}) cells at 10^6 cells/mouse were injected intravenously into the tail vein of 8-week-old NOD/SCID IL2R$_\gamma^{null}$ mice ($n = 10$/group). A, representative radiographs from a mouse in each group at 28 days after injection. Arrows indicate osteolytic "metastatic" lesion. B, osteolytic bone lesions in the spine, femur, tibia, and ulna bones of each mouse were counted using the radiographs. Although both SBC-5 miR-335$^+$ and SBC-5 miR-29a$^+$ xenografts induced fewer osteolytic lesions than controls, the reduction was significant only in miR-335$^+$ xenografts. C, frequency distribution of osteolytic lesions revealed that no lesions developed from 3 SBC-5 miR-335$^+$ xenografts, and the remaining 7 SBC-5 miR-335$^+$ mice exhibited fewer lesions than controls. The number of osteolytic lesions from SBC-5 miR-29a$^+$ xenografts did not differ significantly from control (compared with control, **, $P < 0.01$).

9 mice, respectively (Fig. 3C). The number of osteolytic lesions developed by SBC-5 miR-29a$^+$ xenografts did not differ significantly from SBC-5 Vector^{Ctrl} xenografts (average number of lesions/mouse: 2.3 ± 0.45 vs. SBC-5 Vector^{Ctrl}: 3.3 ± 0.42; $P > 0.05$; Fig. 3).

Downregulation of IGF-IR in SBC-5 miR-335$^+$

We used informatics prediction software (miRanda) to identify insulin-like growth factor-I receptor (IGF-IR) as a potential target of miR-335. Published literature confirmed that IGF-IR was a direct target of miR-335 (32), and its expression correlated with enhanced proliferation, invasion, and migration ability in tumor cells (33, 34) and bone metastases in breast and prostate cancers (35, 36). Western blotting result showed that SBC-5 expressed much higher IGF-IR than SBC-3 cells. In SBC-5 miR-335$^+$, but not in SBC-5 miR-29a$^+$, IGF-IR expression was significantly less than that in SBC-5 Vector^{Ctrl} (Fig. 4).

Downregulation of osteoclast induction and RANKL expression in SBC-5 miR-335$^+$, but not in SBC-5 miR-29a$^+$

First, we assessed the effect of conditioned media from genetically modified SBC-5 cell lines on osteoclast induction *in vitro*. SBC-5 Vector^{Ctrl} CM, increased osteoclast numbers significantly compared with cell-free unconditioned medium (average osteoclast number per well, SBC-5 Vector^{Ctrl} CM: 67.2 ± 5.6 vs. cell-free unconditioned medium: 20.7 ± 3.8 in, $P < 0.001$; Fig. 5A and B). Compared with SBC-5 Vector^{Ctrl} CM, osteoclast induction was reduced by approximately 57% in SBC-5 miR-335$^+$ CM (average 28.7 ± 1.8 osteoclasts per well; $P < 0.001$) and by 24% in miR-29a$^+$ CM (average 49.5 ± 4.8 osteoclasts per well; $P < 0.05$).

Using miRanda software, we identified RANKL, a key cytokine regulating osteoclastogenesis, as a candidate target for miR-335. We found that RANKL expression was higher in cell lysates and culture medium of SBC-5, than that in SBC-3. We confirmed that RANKL expression was significantly reduced in SBC-5 after overexpression of miR-335 (SBC-5 miR-335$^+$), whereas RANKL expression was not different from controls in SBC-5 after overexpression of miR-29a (SBC-5 miR-29a$^+$; Fig. 5C). To show the selectivity of RANKL by miR-335, RANKL 3′UTR was cloned and placed within the 3′UTR of a luciferase reporter expression cassette. Cotransfection in 293TN cells with either the miR-335 expression vector or a control vector showed that miR-335 overexpression significantly reduced luciferase activity of the construct containing the target site of RANKL 3′UTR. When the target sequence was mutated, miR-335 failed to reduce luciferase activity (Fig. 5D and E). These data support the hypothesis that the abrogation or reduction of skeletal osteolysis by SBC-5 miR-335$^+$ xenografts may be attributed, in part, to inhibition of RANKL expression. Collectively, our data support a role for miR-335, but not miR-29a, in the homing of human SCLC SBC-5 cells to bone.

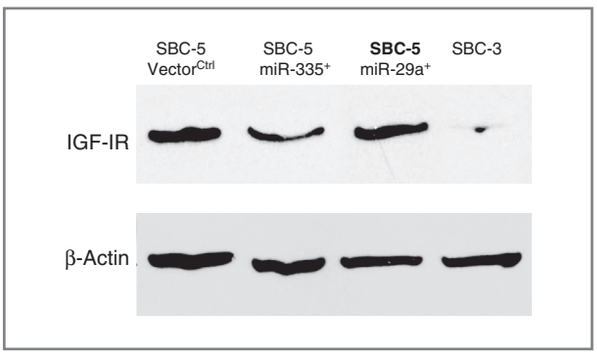

Figure 4. SBC-5 miR-335$^+$, but not SBC-5 miR-29a$^+$, exhibited reduced IGF-IR expression. Serum-starved SBC-5 cell lines (SBC-5 miR-335$^+$, SBC-5 miR-29a$^+$, and SBC-5 Vector^{Ctrl}) and SBC-3 cells were lysed in RIPA buffer, and IGF-IR expression was studied by Western blotting. Compared with SBC-5 Vector^{Ctrl}, IGF-IR expression was lower in SBC-5 miR-335$^+$ and SBC-3 cells, and did not show difference between SBC-5 Vector^{Ctrl} and SBC-5 miR-29a$^+$.

Discussion

Very little is known of the cell and molecular mechanisms underlying the metastatic spread to the skeleton in SCLC. Preclinical studies suggest a role for deregulation of bone turnover because mouse xenograft models of SCLC-induced bone metastases are responsive to bisphosphonate drugs, such as zolendronate, which blunt bone resorption and slow bone turnover (37). Despite their efficacy, bisphosphonates in patients with cancer have been linked to complications such as osteonecrosis of the jaw and bone fractures (38), creating a need for alternate therapies. To investigate alternate molecular regulators of the metastatic spread of SCLC cells to bone, we studied miRNA profiles using human SCLC SBC-5 and SBC-3 cell lines and xenografts in immunodeficient NOD/SCID IL2R$_\gamma^{null}$ mice, and identified miR-335 as putative candidate regulator of RANKL, a key cytokine regulating resorption, and skeletal osteolysis. Confirming the importance of miR-335 as a candidate regulator in metastatic progression, *in vitro* work by others showed that miR-335 overexpression in malignant breast cancer cell xenografts suppressed spread of breast cancer cells to lung and bone (39). Taken together with data in the present study, we hypothesize that miR-335 may be an important regulator of bone metastasis. The work reported here is the first to associate miR-335 with human SCLC, and to link miR-335 with bone metastases of SCLC.

Deregulation of miRNAs has been implicated in carcinogenesis, and miRNAs are being investigated as candidate oncology therapeutic targets for several different types of tumors (40, 41). Multiple loci on chromosome 7 have been previously identified in genetic research on human lung cancer (42), so it is interesting that miR-335 is located in chromosome 7q32.2. In various metastatic breast cancer cell lines, gene deletion and epigenetic promoter hypermethylation of the miR-335 locus on 7q32.2 seemed to be a common feature, resulting in the designation of miR-335 as a "selective metastasis suppressor and tumor initiation suppressor locus in human breast cancer" (43). In breast cancer, expression of miR-335 activated the tumor

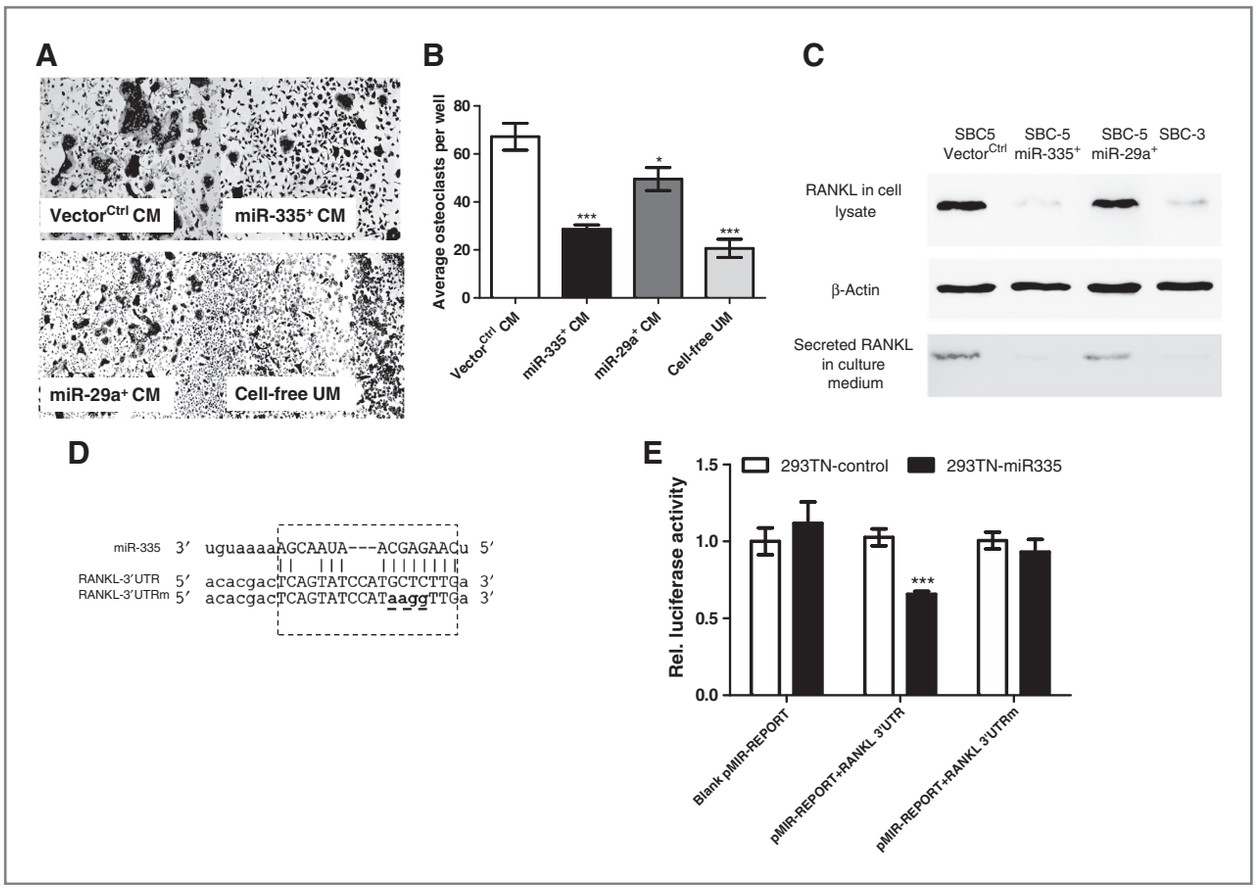

Figure 5. miR-335 targeted RANKL and reduced osteoclast induction in SBC-5. Osteoclasts were induced from murine spleen cells using conditioned medium from each of the SBC-5 cell lines (SBC-5 Vector^{Ctrl}, SBC-5 miR-335^{+}, and SBC-5 miR-29a^{+}) and cell-free unconditioned medium (UM). A, representative osteoclast induction from each group at 7 days after incubation with conditioned media or unconditioned medium. B, SBC-5 Vector^{Ctrl} CM induced more osteoclast formation compared with cell-free unconditioned medium. Osteoclast number was significantly decreased in SBC-5 miR-335^{+} and in SBC-5 miR-29a^{+} compared with SBC-5 Vector^{Ctrl} CM (*, $P < 0.05$; ***, $P < 0.001$; $n = 6$/group, 2 replicate experiments). C, RANKL expression was evaluated in cell lysates and in culture media by Western blotting. RANKL expression was lower in SBC-5 miR-335^{+} and in SBC-3 compared with SBC-5 Vector^{Ctrl} and SBC-5 miR-29a^{+}. D, the 3′UTR of the *RANKL* gene was analyzed by TargetScan and a target sequence for miR-335 was identified. The strategy to make point mutations within the target sequence was listed as RANKL 3′UTRm. E, the miR-335 precursor gene or the control sequence was stably transfected into 293TN cells by lentivirus. These cells were further cotransfected with pMIR reporter vector inserted with RANKL 3′UTR or RANKL 3′UTRm and the pMIR-REPORT β-galactosidase reporter control vector. The Dual Luciferase Assay kit was used in the 3′UTR reporter assay. Overexpression of miR-335 significantly reduced luciferase activity only in cells containing the RANKL 3′UTR, but not in the cells with mutated seed sequence (RANKL 3′UTRm). These results indicated that RANKL 3′UTR was directly targeted by miR-335; compared with control, ***, $P < 0.001$; $n = 3$/group, two replicate experiments).

suppressor gene *BRCA1* via effects on BRCA1 repressor ID4, resulting in increased apoptosis by downregulation of estrogen receptor-α and IGF-IR (32). In gastric cancer cell lines, miR-335 targeted Bcl-w and specificity protein 1, both of which have also been linked to metastatic progression (44). Our data strongly suggest that increased miR-335 may mitigate human metastatic SCLC, but clinical research is needed to validate this speculation, and to determine whether there are common mechanisms regulated by miRNA across cancer types.

We speculated that miR-335 might target cytokines linked to osteoclast induction and bone turnover. We report two cytokines, IGF-IR and RANKL, both of which have been linked to metastases of other cancers (33, 34), were expressed more highly in SBC-5 cells, and were regulated by miR-335. Deregulated IGF-IR may interact with ligand IGFs to stimulate proliferation, invasion, and migration and inhibit apoptosis of cancer cells (33). Breast cancer research has shown that bone-derived IGF-I regulates interactions between bone and breast cancer cells via activation of the IGF-IR/Akt/NF-κB pathway and that IGF-IR knockdown significantly reduced xenograft-induced bone metastases (35). Extending the literature on breast cancer to SCLC, we now show downregulation of IGF-IR in SBC-5 miR-335^{+} correlated with decreased cell proliferation, migration, invasion, and colony formation.

RANKL regulates osteoclast induction, differentiation, survival, and activation (36, 45) and has been implicated in cancer mechanisms (46). Breast cancer and melanoma cell xenografts migrating to bone may stimulate osteoclast

differentiation by RANKL to deregulate bone turnover, resulting in bone resorption and osteolysis (36, 46). Blocking RANKL markedly reduced tumor burden in bones (47). We extended previous reports in breast cancer and lung cancer literature by showing that downregulation of RANKL in SBC-5 miR-335$^+$ markedly reduced osteoclast induction, and that miR-335$^+$ abrogated or reduced skeletal osteolysis induced by miR-335$^+$ xenografts.

Development of NOD/SCID IL2R$_\gamma^{null}$ mice, which lack mature T cells, B cells, and functional NK cells, as xenograft hosts greatly improved the predictability of human tumor xenograft phenotyping for cancer research (48). Using these mice, we reported that skeletal osteolysis was induced within one month of placing SCLC SBC-5 xenografts. SBC-5 miR-335$^+$ abrogated osteolysis in 3 out of 10 mice, and markedly reduced the sites of osteolysis in remaining mice, whereas SBC-5 miR-29a$^+$ had no such effect. These outcomes support our hypothesis that miR-335, but not miR-29a, seems a selective and specific suppressor of bone metastases in this model of SCLC. Our *in vitro* and *in vivo* experiments suggest that miR-335 may be a candidate therapeutic target to mitigate bone metastases in SCLC. Clinical research will be necessary to validate this exciting possibility.

Disclosure of Potential Conflicts of Interest

No potential conflicts of interest were disclosed.

Authors' Contributions

Conception and design: M. Gong, J.M. Hock, X. Yu
Development of methodology: J. Ma, Y. Yang, X. Yu
Acquisition of data (provided animals, acquired and managed patients, provided facilities, etc.): M. Gong, J. Ma, R. Guillemette, M. Zhou
Analysis and interpretation of data (e.g., statistical analysis, biostatistics, computational analysis): M. Gong, Y. Yang, J.M. Hock, X. Yu
Writing, review, and/or revision of the manuscript: M. Gong, R. Guillemette, Y. Yang, J.M. Hock, X. Yu
Study supervision: J.M. Hock, X. Yu

Grant Support

This work was support by grants from the National Natural Science Foundation of China (No. 81072190 to X. Yu, No. 30900244 to M. Gong, No. 81101920 to J. Ma), Science &Technology Department of Sichuan Province (2010SZ0168 to X. Yu), the Ministry of Education of the People's Republic of China [(2011)1139 to X. Yu], Sichuan University (2011SCU04B42 to X. Yu), and U.S. Army Medical Research and Materiel Command research contract USAMRMC (No. 0704400), PI: J.M. Hock.

The costs of publication of this article were defrayed in part by the payment of page charges. This article must therefore be hereby marked *advertisement* in accordance with 18 U.S.C. Section 1734 solely to indicate this fact.

Received March 20, 2013; revised August 6, 2013; accepted August 7, 2013; published OnlineFirst August 21, 2013.

References

1. Cooper S, Spiro SG. Small cell lung cancer: treatment review. Respirology 2006;11:241–8.
2. Ou SH, Ziogas A, Zell JA. Prognostic factors for survival in extensive stage small cell lung cancer (ED-SCLC): the importance of smoking history, socioeconomic and marital statuses, and ethnicity. J Thorac Oncol 2009;4:37–43.
3. Govindan R, Page N, Morgensztern D, Read W, Tierney R, Vlahiotis A, et al. Changing epidemiology of small-cell lung cancer in the United States over the last 30 years: analysis of the surveillance, epidemiologic, and end results database. J Clin Oncol 2006;24:4539–44.
4. Devesa SS, Bray F, Vizcaino AP, Parkin DM. International lung cancer trends by histologic type: male:female differences diminishing and adenocarcinoma rates rising. Int J Cancer 2005;117:294–9.
5. Neal JW, Gubens MA, Wakelee HA. Current management of small cell lung cancer. Clin Chest Med 2011;32:853–63.
6. Demedts LK, Vermaelen KY, van Meerbeeck JP. Treatment of extensive-stage small cell lung carcinoma: current status and future prospects. Eur Respir J 2010;35:202–15.
7. SEER Cancer Statistics Review 1975–2009, Section 15; 2010; Available from: http://seer.cancer.gov/statfacts/html/lungb.html
8. Guise TA. Molecular mechanisms of Osteolytic bone metastases. Cancer 2000;88(12 Suppl):2892–8.
9. Sottnick JL, Keller ET. Understanding and targeting osteoclastic activity in prostate cancer bone metastases. Curr Mol Med 2012;13:626–39
10. Hirsh V, Major PP, Lipton A, Cook RJ, Langer CJ, Smith MR, et al. Zoledronic acid and survival in patients with metastatic bone disease from lung cancer and elevated markers of osteoclast activity. J Thorac Oncol 2008;3:228–36.
11. Mundy GR. Metastasis to bone: causes, consequences and therapeutic opportunities. Nat Rev Cancer 2002;2:584–93.
12. Lim LP, Lau NC, Garrett-Engele P, Grimson A, Schelter JM, Castle J, et al. Microarray analysis shows that some microRNAs downregulate large numbers of target mRNAs. Nature 2005;433:769–73.
13. Zhang B, Pan X, Cobb G, Anderson T. MicroRNAs as oncogenes and tumor suppressors. Dev Biol 2007;302:1–12.
14. Guo H, Ingolia NT, Weissman JS, Bartel DP. Mammalian microRNAs predominantly act to decrease target mRNA levels. Nature 2010;466:835–40.
15. Garzon R, Calin GA, Croce CM. MicroRNAs in Cancer. Annu Rev Med 2009;60:167–79.
16. Ohdaira H, Sekiguchi M, Miyata K, Yoshida K. MicroRNA-494 suppresses cell proliferation and induces senescence in A549 lung cancer cells. Cell Prolif 2012;45:32–8.
17. Kumarswamy R, Mudduluru G, Ceppi P, Muppala S, Kozlowski M, Niklinski J, et al. MicroRNA-30a inhibits epithelial-to-mesenchymal transition by targeting Snai1 and is downregulated in non-small cell lung cancer. Int J Cancer 2012;130:2044–53.
18. Hu H, Li S, Liu J, Ni B. MicroRNA-193b modulates proliferation, migration, and invasion of non–small cell lung cancer cells. Acta Biochim Biophys Sin (Shanghai) 2012;44:424–30.
19. Zhang JG, Guo JF, Liu DL, Liu Q, Wang JJ. MicroRNA-101 exerts tumor-suppressive functions in non-small cell lung cancer through directly targeting enhancer of zeste homolog 2. J Thorac Oncol 2011;6:671–8.
20. Xiong S, Zheng Y, Jiang P, Liu R, Liu X, Chu Y. MicroRNA-7 inhibits the growth of human non-small cell lung cancer A549 cells through targeting BCL-2. Int J Biol Sci 2011;7:805–14.
21. Wang X, Ling C, Bai Y, Zhao J. MicroRNA-206 is associated with invasion and metastasis of lung cancer. Anat Rec (Hoboken) 2011;294:88–92.
22. Li Y, Zhang D, Chen C, Ruan Z, Huang Y. MicroRNA-212 displays tumor-promoting properties in non-small cell lung cancer cells and targets the hedgehog pathway receptor PTCH1. Mol Biol Cell 2012;23:1423–34.
23. Yanaihara N, Caplen N, Bowman E, Seike M, Kumamoto K, Yi M, et al. Unique microRNA molecular profiles in lung cancer diagnosis and prognosis. Cancer Cell 2006;9:189–98.
24. Lee J-H, Voortman J, Dingemanns A, Voeller D, Pham T, Wang Y, et al. MicroRNA expression and clinical outcome of small cell lung cancer. PLoS ONE 2011;6:e21300.
25. Miki T, Yano S, Hanibuchi M, Sone S. Bone metastasis model with multiorgan dissemination of human small-cell lung cancer (SBC-5)

cells in natural killer cell-depleted SCID mice. Oncol Res 2000;12: 209–17.
26. Ma NQ, Liu LL, Min J, Wang JW, Jiang WF, Liu Y, et al. The effect of down regulation of calcineurin Aα by lentiviral vector-mediated RNAi on the biological behavior of small-cell lung cancer and its bone metastasis. Clin Exp Metastasis 2011;28:765–78.
27. Li M, Zhou M, Gong M, Ma J, Pei F, Beamer WG, et al. A novel animal model for bone metastasis in human lung cancer. Oncol Lett 2012; 3:802–6.
28. Livak KJ, Schmittgen TD. Analysis of relative gene expression data using real-time quantitative PCR and the 2(-Delta Delta C(T)) Method. Methods 2001;25:402–8.
29. Granholm S, Lundberg P, Lerner UH. Calcitonin inhibits osteoclast formation in mouse haematopoetic cells independently of transcriptional regulation by receptor activator of NF-{kappa}B and c-Fms. J Endocrinol 2007;195:415–27.
30. Nakamura ES, Koizumi K, Kobayashi M, Saitoh Y, Arita Y, Nakayama T, et al. RANKL-induced CCL22/macrophage-derived chemokine produced from osteoclasts potentially promotes the bone metastasis of lung cancer expressing its receptor CCR4. Clin Exp Metastasis 2006; 23:9–18.
31. Miki T, Yano S, Hanibuchi M, Kanematsu T, Muguruma H, Sone S. Parathyroid hormone-related protein (PTHrP) is responsible for production of bone metastasis, but not visceral metastasis, by human small cell lung cancer SBC-5 cells in natural killer cell-depleted SCID mice. Int J Cancer 2004;108:511–5.
32. Heyn H, Engelmann M, Schreek S, Ahrens P, Lehmann U, Kreipe H, et al. MicroRNA miR-335 is crucial for the BRCA1 regulatory cascade in breast cancer development. Int J Cancer 2011;129:2797–806.
33. Riedemann J, Macaulay VM. IGF1R signalling and its inhibition. Endocr Relat Cancer 2006;13 Suppl 1:S33–43.
34. Stracke ML, Engel JD, Wilson LW, Rechler MM, Liotta LA, Schiffmann E. The type I insulin-like growth factor receptor is a motility receptor in human melanoma cells. J Biol Chem 1989;264: 21544–9.
35. Hiraga T, Myoui A, Hashimoto N, Sasaki A, Hata K, Morita Y, et al. Bone-derived IGF mediates crosstalk between bone and breast cancer cells in bony metastases. Cancer Res 2012;72:4238–49
36. Yin JJ, Pollock CB, Kelly K. Mechanisms of cancer metastasis to the bone. Cell Res 2005;15:57–62.
37. Green JR, Clezardin P. Mechanisms of bisphosphonate effects on osteoclasts, tumor cell growth, and metastasis. Am J Clin Oncol 2002; 25:S3–9.
38. Biasotto M, Chiandussi S, Dore F, Rinaldi A, Rizzardi C, Cavalli F, et al. Clinical aspects and management of bisphosphonates-associated osteonecrosis of the jaws. Acta Odontol Scand 2006;64:348–54.
39. Tavazoie SF, Alarcon C, Oskarsson T, Padua D, Wang Q, Bos PD, et al. Endogenous human microRNAs that suppress breast cancer metastasis. Nature 2008;451:147–52.
40. Lu J, Getz G, Miska EA, Alvarez-Saavedra E, Lamb J, Peck D, et al. MicroRNA expression profiles classify human cancers. Nature 2005; 435:834–8.
41. Stenvang J, Silahtaroglu AN, Lindow M, Elmen J, Kauppinen S. The utility of LNA in microRNA-based cancer diagnostics and therapeutics. Semin Cancer Biol 2008;18:89–102.
42. Campbell J, Lockwood WW, Buys TP, Chari R, Coe BP, Lam S, et al. Integrative genomic and gene expression analysis of chromosome 7 identified novel oncogene loci in non-small cell lung cancer. Genome 2008;51:1032–9.
43. Kim K, Yoshida M, Zhang X, Shu W, Lee H, Rimner A, et al. MicroRNA-335 inhibits tumor reinitiation and is silenced through genetic and epigenetic mechanisms in human breast cancer. Genes Dev 2011;25: 226–31.
44. Xu Y, Zhao F, Wang Z, Song Y, Luo Y, Zhang X, et al. MicroRNA-335 acts as a metastasis suppressor in gastric cancer by targeting Bcl-w and specificity protein 1. Oncogene 2012;31:1398–407.
45. Teitelbaum SL, Ross FP. Genetic regulation of osteoclast development and function. Nat Rev Genet 2003;4:638–49.
46. Huang L, Cheng YY, Chow LT, Zheng MH, Kumta SM. Tumour cells produce receptor activator of NF-kappaB ligand (RANKL) in skeletal metastases. J Clin Pathol 2002;55:877–8.
47. Jones DH, Nakashima T, Sanchez OH, Kozieradzki I, Komarova SV, Sarosi I, et al. Regulation of cancer cell migration and bone metastasis by RANKL. Nature 2006;440:692–6.
48. Brehm MA, Shultz LD, Greiner DL. Humanized mouse models to study human diseases. Curr Opin Endocrinol Diabetes Obes 2010;17:120–5.